Structural basis for enhanced MHET degrading activity of engineered feruloyl esterase

P. Karampa[1], K. Makryniotis[2], E. Nikolaivits[2], E. Topakas[2], V. Daskalakis[3], M. Dimarogona[1]*

[1] Laboratory of Structural Biology and Biotechnology, Department of Chemical Engineering, University of Patras, Patras, Greece,
[2] Industrial Biotechnology & Biocatalysis Group, Biotechnology Laboratory, School of Chemical Engineering, National Technical University of Athens, Athens, Greece,
[3] Laboratory of Biomolecular Dynamics and Engineering, Department of Chemical Engineering, University of Patras, Patras, Greece
(* mdimarog@chemeng.upatras.gr)

Introduction

Enzymatic degradation offers a promising solution to the persistent accumulation of synthetic plastics in the environment [1]. Poly(ethylene terephthalate) (PET) hydrolases (PETases) cleave the ester bonds of the polymer, producing mono-(2-hydroxyethyl) terephthalate (MHET), as primary degradation product [2]. MHET hydrolases (MHETases) further cleave MHET into terephthalic acid (TPA) and ethylene glycol, enabling their reuse as chemical feedstocks. Ferulic acid esterases (E.C. 3.1.1.73, FAEs) are a class of esterases with biotechnological relevance, as they can hydrolyze the ester linkages between hydroxycinnamic acids and arabinose in the plant cell walls. A FAE from *Fusarium oxysporum* (*Fo*FaeC, PDB ID: 6FAT) [3], belonging to the tannase-like family, is a structural homolog of the bacterial MHETase from *Ideonella sakaiensis* (PDB ID: 6JTT), [4,5]. *Fo*FaeC shows activity on PET oligomers and acts synergistically with PETases to enhance PET degradation [6].

In this study, we present:

1. The **crystal structure of an *Fo*FaeC variant, *Fo*FaeC_G122S,** engineered by structure-guided mutagenesis to mimic the MHETase active site.
2. The crystal structure of *Fo*FaeC_G122S in complex with benzoic acid (BA).
3. Molecular Dynamics (MD) and Docking Simulations of both the wild-type *Fo*FaeC and its variant.

1. Crystal structure of *Fo*FaeC_G122S

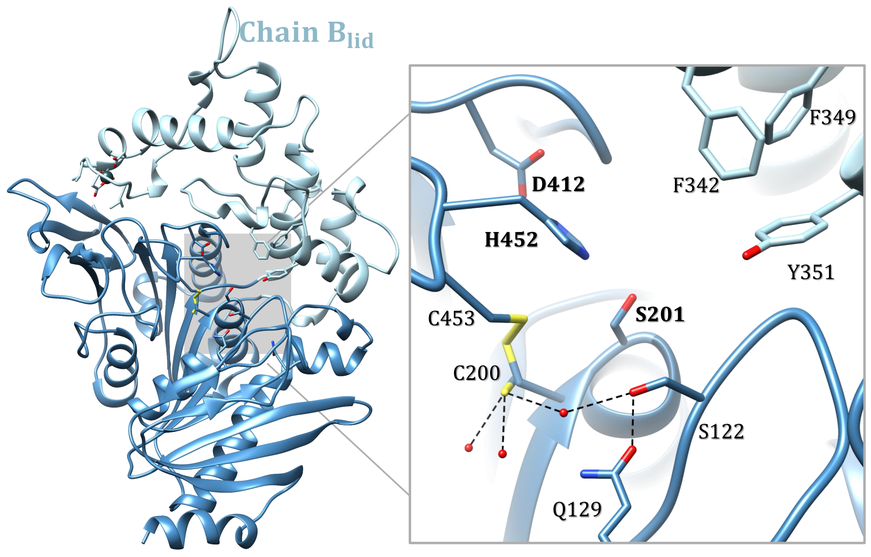

Figure 1. Cartoon representation of *Fo*FaeC_G122S monomer (PDB ID: 9I50, molecule B). It is composed of an α/β hydrolase domain (steel blue) and an α-helical lid domain composed of residues 229-389 (light blue). The engineered Ser122 introduced the formation of a hydrogen bond between Ser122 and Gln129.

Chain B$_{Hydrolase}$

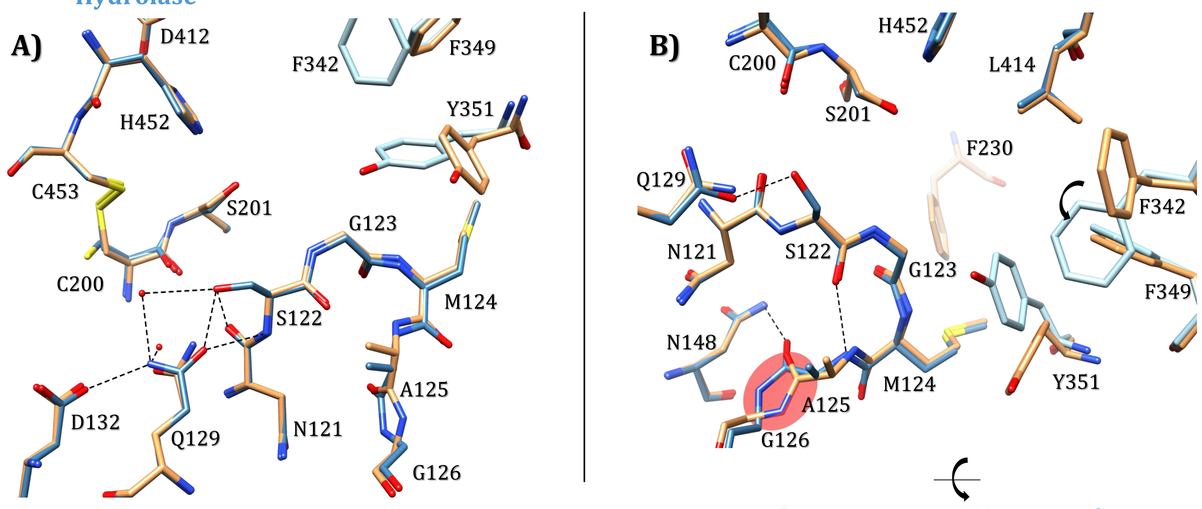

Figure 2. *Fo*FaeC_G122S superimposed on the *Fo*FaeC (PDB ID: 6FAT). Close-up view of the mutation region of *Fo*FaeC_G122S, with hydrogen bonds formed between the engineered Ser122 and Gln129, as well as between Gln129 and Asp132. A) Stick representation of the *cis*/*trans* conformation between Ala125 – Gly126, highlighting the closed/open conformation of Phe342. The hydrogen bonds shown in dashed black lines correspond to the *Fo*FaeC_G122S structure.

2. *Fo*FaeC_G122S in complex with benzoic acid

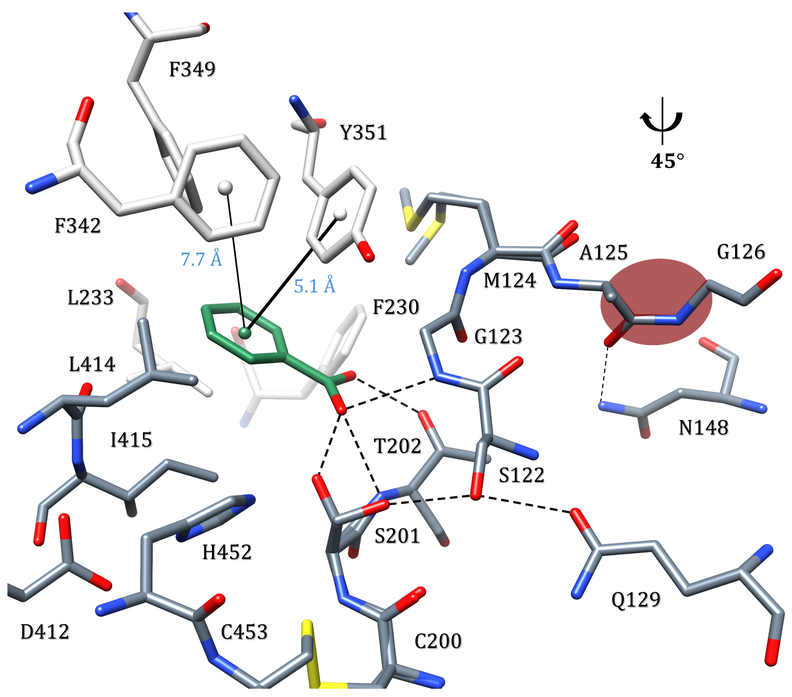

Figure 3. Crystal structure of *Fo*FaeC_G122S in complex with benzoic acid (PDB ID: 9HUN). Close-up view of the substrate binding site. The catalytic triad (Ser201-His452-Asp412) and the hydrophobic environment (Phe230, Leu233, Phe342, Phe349, Tyr351, Leu414, Ile415) are shown as sticks. The side chain of Phe342 is in an already flipped conformation

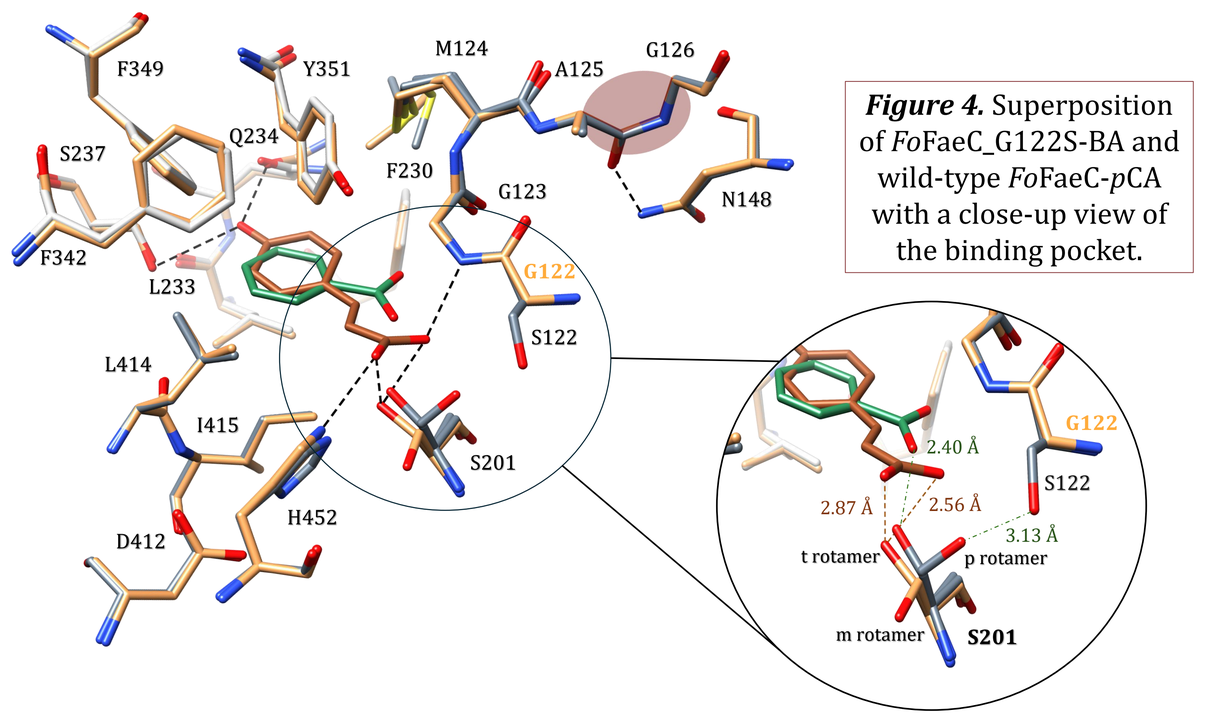

Figure 4. Superposition of *Fo*FaeC_G122S-BA and wild-type *Fo*FaeC-*p*CA with a close-up view of the binding pocket.

3. Molecular dynamics and Docking simulations

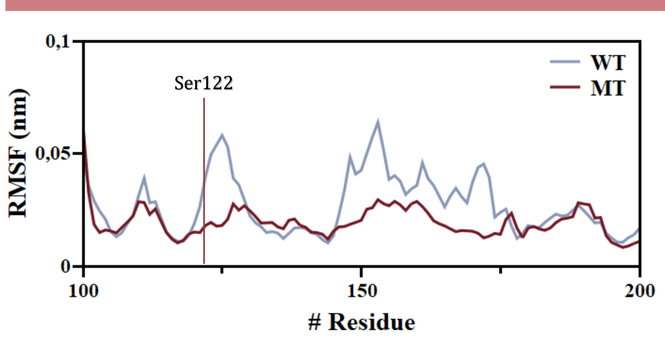

Figure 5. Comparison between Root Mean Square Fluctuation (RMSF) of wild-type *Fo*FaeC (WT) and mutant *Fo*FaeC_G122S (MT) focusing on the region of mutation along 0.5μs MD simulation.

Table 1. Average free binding energies (ΔG) and dissociation constants (K_D) of WT and MT after docking simulations performed with YASARA 21.6.17.

Structure	ΔG (kcal mol^{-1})	K_D (mM)
WT - MHET	5.068 ± 0.321	0.229 ± 0.147
MT - MHET	5.153 ± 0.208	0.178 ± 0.066

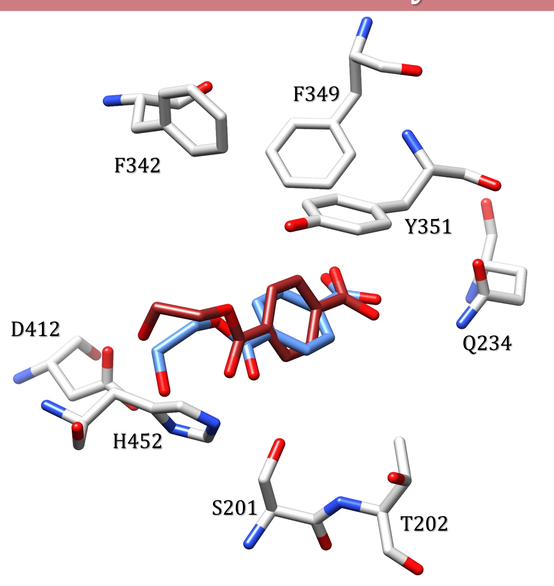

Figure 6. Superposition of WT (blue) and MT (red) structures after docking simulations with MHET. Key conformations for WT and MT were obtained from the k-means clustering analysis over MD trajectories.

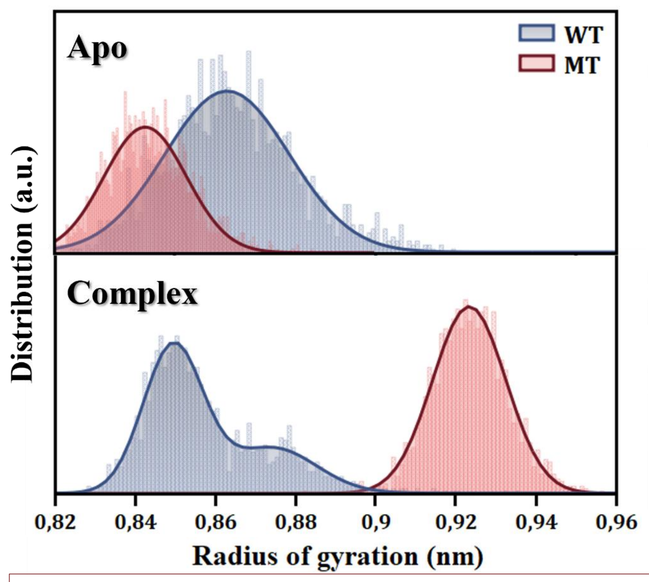

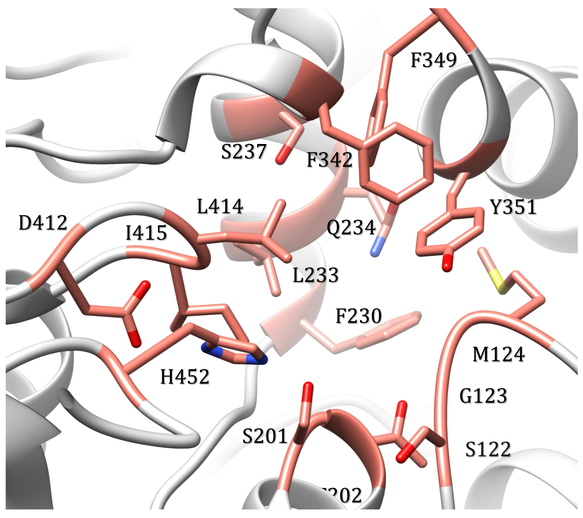

Figure 7. Radius of gyration (R_g) were calculated by the backbone atoms of the binding pocket residues over 0.5μs MD simulation of the apo and MHET-bound forms. Binding pocket residues used for the R_g calculation are shown in pink stick representation.

Conclusions

- Ser122 stabilizes the mutated region by forming hydrogen bonds with Gln129.
- The movement of the Phe342 side chain and the *cis-trans* alteration of 125-126 peptide bond indicate that the mutation induces a structural rearrangement of the enzyme's active site, making it resemble to ligand-bound state.
- *Fo*FaeC_G122S exhibits an approximately 2 Å increase in binding pocket cavity size upon MHET binding, indicating a pocket expansion that could accommodate larger substrates.
- **The structural analysis sheds light on the molecular characteristics that append improved properties to the engineered enzyme, contributing to the design of robust biocatalysts for plastic recycling.**

Acknowledgments

We would like to thank the staff at beamlines P13 (PETRA III, EMBL Hamburg) for help during data collection and iNEXT Discovery for providing financial support for synchrotron data collection. The simulations were performed on the Luxemburg national supercomputer MeluXina. V.D. gratefully acknowledges the LuxProvide teams for their expert support. The research work was supported by the Hellenic Foundation for Research and Innovation (H.F.R.I.) under the National Recovery and Resilience Plan (Greece 2.0) Action, under the "Sub-action II Funding Projects in Leading-Edge Sectors" (EnZyReMix, project number: 15024). This work was also supported by COST Action CA21162, supported by COST (European Cooperation in Science and Technology, https://www.cost.eu/).

References

[1] Urbanek et al. (2021) *Front Bioeng Biotech.*, 9, 771133. [2] Yoshida et al. (2021) *Meth Enzym.*, 687, 9, 187-205. [3] Dimarogona et al. (2020) *FEBS Let.*, 594, 1738-1749. [4] Ferousi et al. (2023) *FEBS Let.*, 597, 1415-1427. [5] Sagong et al. (2020) *ACS Cat.*, 10, 4805-4812. [6] Makryniotis et al. (2025) *Int. J. Bion. Macromol.*, 333, 148892.